Ab initio thermodynamics of $Ba_cSr_{(1-c)}TiO_3$ solid solutions

D. Fuks,[1] S. Dorfman,[2] S. Piskunov,[3,4] and E. A. Kotomin[3,5]
[1]*Materials Engineering Department, Ben-Gurion University of the Negev, POB 653, Beer-Sheva, Israel*
[2]*Department of Physics, Israel Institute of Technology-Technion, 32000 Haifa, Israel*
[3]*Institute for Solid State Physics, University of Latvia, Kengaraga 8, LV-1063 Riga, Latvia*
[4]*Fachbereich Physik, Universität Osnabrück, Barbarastraße 7, D-49069 Osnabrück, Germany*
[5]*Max-Planck-Institut für Festkörperforschung, Heisenbergstraße 1, D-70569 Stuttgart, Germany*
(Received 12 March 2004; revised manuscript received 25 October 2004; published 19 January 2005)

Based on *ab initio* calculations for a number of the $Ba_cSr_{(1-c)}TiO_3$ (BST) superlattices, we developed a thermodynamic approach to these solid solutions. In particular, we calculate the BST phase diagram and show that at relatively low temperatures (below 400 K for $c=0.5$ and 300 K for $c=0.1$) the spinodal decomposition of the solid solution occurs. As a result, we predict for small Ba concentrations formation of $BaTiO_3$ nanoregions in a predominantly $SrTiO_3$ matrix and vice versa, which is confirmed by the Raman, polarization, ultrasonic, neutron diffraction, and diffusion experiments.

DOI: 10.1103/PhysRevB.71.014111 PACS number(s): 64.75.+g, 64.60.−i

I. INTRODUCTION

In the last decade complex perovskite solid solutions with a common formula $(A,A',A'',\ldots)(B,B',B'',\ldots)O_3$ have attracted growing attention because of numerous unusual and sometimes unexpected properties. These properties have opened important fields for such material applications, stimulating further efforts in the study of their behavior under different conditions. It is well recognized nowadays that the dielectric and piezoelectric properties, response on external excitations, etc., in these solid solutions are linked to the structural properties, including compositional ordering and formation of complicated heterostructures.[1–6]

For $Ba_cSr_{(1-c)}TiO_3$ (BST) solid solutions in the Ba-rich region ($c>0.5$), the dielectric anomalies were associated with the fluctuations of the order parameter.[7] The dielectric and ultrasonic study on Sr-rich BST was reported.[8] It was shown there that a small addition of Ba to $SrTiO_3$ leads to formation of a glassy state and complicates significantly the sequence of phase transitions observed at $c\approx 0.15$. Structural evolution and polar order in BST was reported,[9] being based on the combination of neutron diffraction and diffusion, high-resolution x-ray experiments, as well as dielectric susceptibility and polarization measurements. It was shown that the Ba-critical concentration exists, $c_{cr}\approx 0.094$, which separates the *phase diagram* (PD) into two regions: a solely antiferrodistortive (AFD) phase transition ($c<c_{cr}$) and the sequence of three $BaTiO_3$-type ferroelectric phase transitions ($c>c_{cr}$). Moreover, inside the nonferroelectric AFD phase a local polarization is observed, with the magnitude comparable to the values of spontaneous polarization in the ferroelectric phases of the Ba-rich compounds. The results of Raman study of BST films with the thickness of ~ 1 μm and with Ba atomic fraction $c=0.05$, 0.1, 0.2, 0.35, and 0.5 (Ref. 10) show the striking similarity with the behavior of relaxor ferroelectrics, which was explained by the existence of polar nanoregions in the BST thin films.

In order to describe and explain the link between the structural and dielectric properties in ferroelectric solid solutions, significant efforts were made. A simple, purely ionic model, which accounts for electrostatic interaction, was presented[11] and aimed to reproduce the compositional long-range order observed in a large class of perovskite solid solutions. To go beyond the ground-state behavior and to make conclusions on thermodynamic behavior as a function of the temperature, the Metropolis Monte Carlo simulations were further carried out. However, this model does not allow ordering in isovalent binary solid solutions. To describe the weak order in $Pb(Mg,Nb)O_3$ (PMN), for example, it was necessary to account for the multivalent nature of Pb atoms. Accounting for a charge transfer may be accomplished using direct computer modeling in the framework of the electrostatic model[12] or may be carried out by means of *ab initio* calculations. A comparative study of $Pb(B,B')O_3$ and $Ba(B,B')O_3$ perovskites was performed[13] on the basis of plane-wave pseudopotential calculations, and the trends of the low-temperature disordering in $Pb(B,B')O_3$ as compared with $Ba(B,B')O_3$ were discussed. It was shown that the long-range Coulomb interactions that drive B-site ordering in Ba systems do not dominate in Pb systems. Efforts were made to study the finite-temperature properties of some isovalent perovskite solid solutions (see, for example, Refs. 14–16). These theoretical papers deal mostly with the description of the ferroelectric phase transformations based on the effective Hamiltonians. In particular, the virtual crystal approximation (VCA), which has well-known disadvantages,[17] including lack of solid fundamental background, was used.[15,16] In Ref. 15 as many as 18 parameters of the effective Hamiltonian were fitted to the results of VCA calculations. In several studies artificially constructed and quite arbitrary chosen superstructures were used to model disordered solid solutions.[18,19] Lastly, molecular dynamics (MD) calculations have been also performed.[20] Although the giant dielectric constant in BST for $c=0.7$ was explained there, other above-mentioned fine features of the phase transitions were not found. On the one hand, this clearly demonstrates the importance of *ab initio* calculations for perovskite alloys, but on the other hand, raises the question of how to

explain the peculiarities of phase transitions in complex BST alloys without compositional long-range order. A rather short but comprehensive review of the very recent use of first-principle-derived approaches to piezoelectricity in simple and complex ferroelectric perovskites was presented in Ref. 21.

There is great interest in the study of this system in the whole $0<c<1$ range of atomic substitutions at low temperatures where phase transitions occur. Unfortunately, the experimental PDs for BST solid solutions are known only for high temperatures, 1538–1703 K (Ref. 22). A complete picture of the whole PD is still lacking although much experiment data indicate peculiarities of the low-temperature phase transitions in $Ba_cSr_{(1-c)}TiO_3$ where the composition varies widely.

In this paper, we show that the statistical thermodynamic approach combined with the *ab initio* Hartree-Fock calculations allows us to predict the main features of the quasibinary PD for the BST solid solutions in a wide range of Ba concentrations and, thus, to shed some light on the complicated picture of phase transitions in this system. Our results clearly demonstrate that fine peculiarities of these transitions at relatively low temperatures arise due to *spinodal decomposition*. Formation of specific morphology of solid solutions, which differs essentially in the region between the solvus and spinodal and below the spinodal, enables us to explain unusual behavior of both $SrTiO_3$ slightly doped by Ba and Ba-rich solid solutions.

Our method allows us to avoid numerous and not well-justified approximations commonly used in quantum-mechanical calculations, simulating disordered or partly ordered solid solutions. In particular, we perform the calculations *only for ordered superstructures* and use these results for extracting the key energy parameter that is necessary for the thermodynamic analysis of the BST solid solution. Unlike many previous approaches, our theory has no fitting parameters.

The paper is organized as follows. Section II deals with the short description of the statistical thermodynamic approach and its application to quasibinary $Ba_cSr_{(1-c)}TiO_3$ solid solutions. Here we also define different superstructures for which *ab initio* Hartree-Fock calculations are performed. Some computational details are given in Sec. III. In Section IV we show how, based on the calculated energy data for ordered superstructures, we predict the PD of the considered system and discuss the consequences of the obtained decomposition tendencies. Section V concludes the paper.

II. THERMODYNAMIC THEORY

We develop here a statistical thermodynamic approach for modeling the formation of BST solid solutions to be combined with *ab initio* atomistic calculations. Periodic-structure *ab initio* calculations of the BST electronic structure, which we use here, are applicable only for the absolutely ordered structures. This requires us to formulate the problem in such a way that allows us to extract the necessary energy parameters from the calculations for the ordered phases and then to apply these parameters to the study of the disordered or partly ordered solid solutions in order to get the information on the thermodynamic behavior of the BST solid solution. From our microscopic study and experiment data,[19] it follows that in the perovskite alloy $Ba_cSr_{(1-c)}TiO_3$ the Ba atoms substitute for Sr at all atomic fractions, $0<c<1$. This allows us to focus only on the alloying sublattice, similar to Ref. 11, and to consider the solid solutions of these components on the sites of simple cubic lattice immersed in the external field of the remaining Ti and O ions and in the field of the electronic charge distribution created by these atoms. When the atomic fraction of Ba changes, this may affect the external field and changes the charge distribution. This is accounted in the Hartree-Fock calculations. The thermodynamics of such *quasibinary* solid solutions may be formulated in terms of the *effective mixing interatomic potential*

$$\tilde{V}(\vec{r},\vec{r}') = V_{AA}(\vec{r},\vec{r}') + V_{BB}(\vec{r},\vec{r}') - 2V_{AB}(\vec{r},\vec{r}'), \qquad (1)$$

where $V_{AA}(\vec{r},\vec{r}')$, $V_{BB}(\vec{r},\vec{r}')$, and $V_{AB}(\vec{r},\vec{r}')$ are the effective interatomic potentials between Ba atoms (A), between Sr atoms (B), and between Ba and Sr atoms, respectively; $\vec{r}$ and $\vec{r}'$ are the positions of the sites in the simple cubic lattice. The *effective* mixing interatomic potential [Eq. (1)] describes the interactions of A and B components in such a system in the field of the remaining atoms in the perovskite solid solution.

The atomic fractions of Ba or Sr atoms in this simple cubic solid solution can be determined in the usual way. The total number of particles in this system is conserved, being equal to the number of simple cubic lattice sites. This simplifies the application of a traditional thermodynamic theory of substitutional solid solutions. The analysis of thermodynamic stability of this solid solution turns into a study of the ordering and/or decomposition tendencies of such a binary system. Its stability may be considered in terms of the PD of the $Ba_cSr_{(1-c)}TiO_3$ alloy. We use the concentration wave (CW) approach,[24] which has several advantages over other statistical theories of alloys. One such advantage is that the CW theory is based on the Fourier transforms of interatomic interaction potentials. Thus, it accounts for, formally, the interactions in *all* coordination shells, i.e., avoiding the usual approximation of the first or first and second, etc., nearest-neighbor interactions.

In this theory, the distribution of atoms A in a binary A-B alloy is described by a single *occupation probability function* $n(\vec{r})$. This function provides the probability of finding the atom A (Ba) at the site $\vec{r}$ of the crystalline lattice. The configurational part of the *free-energy* formation of a solid solution per atom is given by

$$F = \frac{1}{2N}\sum_{\substack{\vec{r},\vec{r}' \\ \vec{r}\neq\vec{r}'}} \tilde{V}(\vec{r},\vec{r}')n(\vec{r})n(\vec{r}') + kT\sum_{\vec{r}}\{n(\vec{r})\cdot\ln n(\vec{r}) + [1-n(\vec{r})]\cdot\ln[1-n(\vec{r})]\}. \qquad (2)$$

The summation in Eq. (2) is performed over the sites of the Ising lattice (a simple cubic lattice in our case) with Ba and Sr atoms distributed on it. The function $n(\vec{r})$ that determines the distribution of solute atoms in the ordering phase may be

expanded into the Fourier series. It is presented as a superposition of CWs

$$n(\vec{r}) = c_A + \frac{1}{2}\sum_{j_s,s}[Q(\vec{k}_{j_s})e^{i\vec{k}_{j_s}\vec{r}} + Q*(\vec{k}_{j_s})e^{-i\vec{k}_{j_s}\vec{r}}], \qquad (3)$$

where c_A is a concentration of particles A, $e^{i\vec{k}_{j_s}\vec{r}}$ is a CW, $\vec{k}_{j_s}$ is a nonzero wave vector defined in the first Brillouin zone (BZ) for the Ising lattice of the disordered solid solution, the index $\{j_s\}$ numerates the wave vectors in the BZ, which belong to the star s, and $Q(\vec{k}_{j_s})$ is the CW amplitude. As shown in Ref. 24, all $Q(\vec{k}_{j_s})$ are linear functions of the long-range-order (LRO) parameters of the superlattices that may be formed on the basis of the Ising lattice of the disordered solid solution

$$Q(\vec{k}_{j_s}) = \eta_s \gamma_s(j_s). \qquad (4)$$

Here the η_s are the LRO parameters, and the $\gamma_s(J_s)$ are coefficients that determine the symmetry of the site-occupation probabilities $n(\vec{r})$ (the symmetry of the superstructure) with respect to rotation and reflection symmetry operations. The LRO parameters are defined in such a way that they are equal to unity in a completely ordered state, where the occupation probabilities $n(\vec{r})$ on all the lattice sites $\{\vec{r}\}$ are either unity or zero. This requirement completely defines the constants $\gamma_s(j_s)$. This definition of the LRO parameters coincides with the conventional definition in terms of the occupation probabilities of sites in the different sublattices. Substitution of Eqs. (3) and (4) into the first term of Eq. (2) gives the *internal formation energy* (per atom) for the ordered superstructure

$$\Delta U = \frac{1}{2}\tilde{V}(0)\cdot c_A^2 + \frac{1}{2}\sum_{s,j_s}\gamma_s^2(j_s)\eta_s^2\tilde{V}(\vec{k}_{j_s}), \qquad (5)$$

where $\tilde{V}(\vec{k}_{j_s})$ is the Fourier transform of the mixing interatomic potential and $\tilde{V}(0)$ is the same for the $\vec{k}_{j_s}=0$. It may be shown that the $V(\vec{k}_{j_s})$ remains the same for different vectors $\vec{k}_j$ belonging to the same star of vectors. Equations (2) and (5) define the *Helmholtz free energy* and internal energy of the ordered phases with respect to the reference state.

For simulating the superstructures in quasibinary solid solution, we used the structures given in Fig. 1. This choice of superstructures is not arbitrary and not based on any specific type of interatomic interactions. Obviously, it is impossible to calculate all the possible structures that may, in principle, exist in the solid solution. We decided, thus, to limit our study to those structures that are stable with respect to the formation of anti-phase domains. Criteria that we used to construct these superstructures are independent on the type of interatomic interactions but based purely on the symmetry considerations that have been well known since the early papers of Lifshitz.[25] The discussion on this subject is included into a classic book.[26]

Site occupation probabilities for these structures are presented in the form of Eq. (3). They are found with the determination of vectors $\vec{k}_{j_s}$. The superstructure vectors $\vec{k}_{j_s}$ define

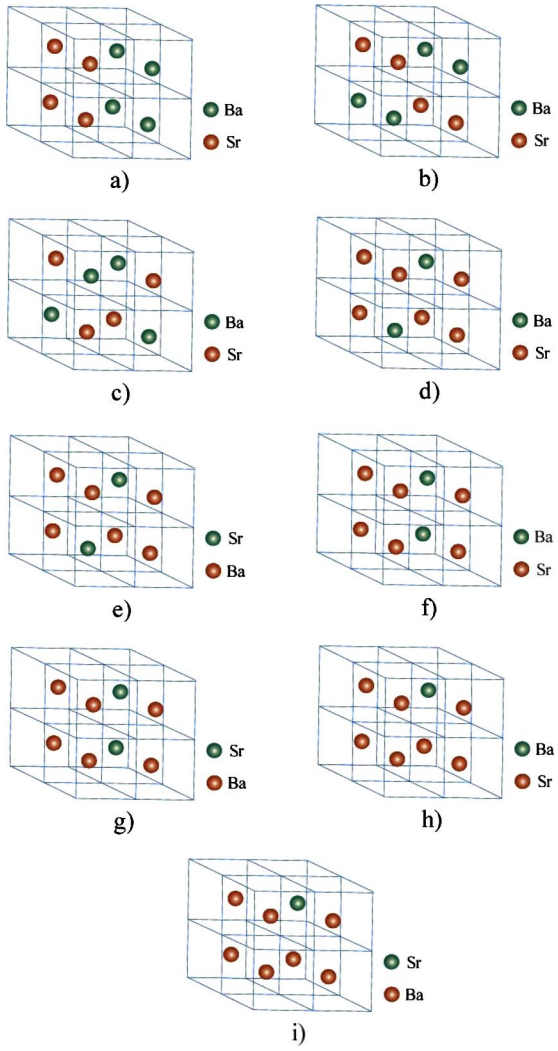

FIG. 1. Superstructures *a* to *i* in quasibinary $Ba_cSr_{1-c}TiO_3$ solid solutions used in *ab initio* calculations.

the positions of the additional x-ray reflections that appear when the binary system changes from a disordered state on the Ising lattice to an ordered or partly ordered state. The vector $\vec{k}_{j_s}$ determines new unit translations in the reciprocal lattice arising from the reduction of the translation symmetry caused by the ordering. To choose these vectors, the Lifshitz criterium[25,26] is used. According to this criterium, the point group of the vector $\vec{k}_{j_s}$ contains the intersecting elements of symmetry. The stars of vectors $\vec{k}_{j_s}$ for the simple cubic lattice are

$$\begin{aligned} &1)\ \left(\tfrac{1}{2},0,0\right),\left(0,\tfrac{1}{2},0\right),\left(0,0,\tfrac{1}{2}\right);\\ &2)\ \left(\tfrac{1}{2},\tfrac{1}{2},0\right),\left(\tfrac{1}{2},0,\tfrac{1}{2}\right),\left(0,\tfrac{1}{2},\tfrac{1}{2}\right);\\ &3)\ \left(\tfrac{1}{2},\tfrac{1}{2},\tfrac{1}{2}\right). \end{aligned} \qquad (6)$$

These vectors are given in the units $(2\pi/a)$ where a is the cubic lattice parameter. All possible ordered structures on the simple cubic lattice that satisfy the Lifshitz criterium are dis-

TABLE I. Site-occupation probabilities $n(\vec{r})$, stoichiometric compositions c_{st}, and the energies of formation ΔU, for the ordering phases in $Ba_cSr_{(1-c)}TiO_3$ solid solutions. $\tilde{V}_1$, $\tilde{V}_2$, and $\tilde{V}_3$ are the Fourier transforms of the mixing potential in the $\vec{k}_{j_s}$ points that correspond to the stars 1, 2, and 3, Eq. (6).

	$n(\vec{r})$	c_{st}	γ	ΔU
1	$c+\gamma\eta_1 e^{i\pi z}$	$\frac{1}{2}$	$\frac{1}{2}$	$\frac{1}{2}\tilde{V}(0)c^2+\frac{1}{8}\tilde{V}_1\eta_1^2$
2	$c+\gamma\eta_2 e^{i\pi(x+y)}$	$\frac{1}{2}$	$\frac{1}{2}$	$\frac{1}{2}\tilde{V}(0)c^2+\frac{1}{8}\tilde{V}_2\eta_2^2$
3	$c+\gamma\eta_3 e^{i\pi(x+y+z)}$	$\frac{1}{2}$	$\frac{1}{2}$	$\frac{1}{2}\tilde{V}(0)c^2+\frac{1}{8}\tilde{V}_3\eta_3^2$
4	$c+\gamma\eta_2[e^{i\pi(x+y)}+e^{i\pi(x+z)}+e^{i\pi(y+z)}]$	$\frac{1}{4}$	$\frac{1}{4}$	$\frac{1}{2}\tilde{V}(0)c^2+\frac{3}{32}\tilde{V}_2\eta_2^2$
		$\frac{3}{4}$	$-\frac{1}{4}$	
5	$c+\gamma_1\eta_1[e^{i\pi x}+e^{i\pi y}]+\gamma_2\eta_2 e^{i\pi(x+y)}$	$\frac{1}{4}$	$\gamma_1=\gamma_2=\frac{1}{4}$	$\frac{1}{2}\tilde{V}(0)c^2+\frac{1}{16}\tilde{V}_1\eta_1^2+\frac{1}{32}\tilde{V}_2\eta_2^2$
		$\frac{3}{4}$	$\gamma_1=-\gamma_2=-\frac{1}{4}$	
6	$c+\gamma\eta_1[e^{i\pi x}+e^{i\pi y}+e^{i\pi z}]+$ $\gamma_2\eta_2[e^{i\pi(x+y)}+e^{i\pi(x+z)}+e^{i\pi(y+z)}]+$ $\gamma_3\eta_3 e^{i\pi(x+y+z)}$	$\frac{1}{8}$	$\gamma_1=\gamma_2=\gamma_3=\frac{1}{8}$	$\frac{1}{2}\tilde{V}(0)c^2+\frac{3}{128}\tilde{V}_1\eta_1^2$
		$\frac{7}{8}$	$\gamma_1=\gamma_2=\gamma_3=-1/8$	$+\frac{3}{128}\tilde{V}_2\eta_2^2+\frac{1}{128}\tilde{V}_3\eta_3^2$

played in Fig. 1. Figs. 1(a)–1(c) show the structures that are described by the single vector $\vec{k}_{j_s}$. In particular, the superstructure vector $\vec{k}_{3_1}=(2\pi/a)(0,0,\frac{1}{2})$ defines the structure in Fig. 1(a). The vector $\vec{k}_{1_2}=(2\pi/a)(\frac{1}{2},\frac{1}{2},0)$ defines the structure shown in Fig. 1(b), while the vector $\vec{k}_{1_3}=(2\pi/a)\times(\frac{1}{2},\frac{1}{2},\frac{1}{2})$ defines the structure in Fig. 1(c). The superstructure in Fig. 1(e) is described, for example, by a combination of *three* CWs with vectors $\vec{k}_{j_s}$,

$$\vec{k}_{1_1}=\frac{2\pi}{a}\left(\frac{1}{2},0,0\right),\vec{k}_{2_1}=\frac{2\pi}{a}\left(0,\frac{1}{2},0\right),\text{ and }\vec{k}_{1_2}=\frac{2\pi}{a}\left(\frac{1}{2},\frac{1}{2},0\right).$$

The site occupation probabilities for structures in Fig. 1 are presented in Table I together with the stoichiometric compositions and the formation energies for these phases ΔU with respect to the heterophase mixture, $c\mathrm{BaTiO_3}+(1-c)\mathrm{SrTiO_3}$. This mixture is assumed to serve as the standard state. Table I contains a comprehensive list of the binary superstructures that may be formed on the simple cubic lattice and are stable with respect to the formation of antiphase boundaries,[27] according to the Lifshitz criterium. In Table I, x and y are the coordinates of the lattice sites on the Ising lattice (in the lattice parameter units). It is easy to check by a direct substitution of coordinates of the simple cubic lattice sites that, for the displayed ordered structures and stoichiometric compositions, the occupation probabilities are equal to unity on the Ba sites and are zero on the Sr sites.

III. COMPUTATIONAL DETAILS

To perform *ab initio* calculations, we use the CRYSTAL-98 computer code.[28–30] This is a periodic-structure computer program, using the linear combination of atomic orbitals (LCAO) basis set (BS). Its main advantage is the ability to calculate the electronic structure using both Hartree-Fock (HF) and Kohn-Sham (KS) Hamiltonians or various density-functional-theory–HF (DFT-HF) *hybrid approximations* using the identical BS and other computational parameters. In present simulations we employ the effective core pseudopotentials (ECPs). This approximation allows us to account for the chemically inert core electrons with the effective pseudopotentials and, hence, to focus more on calculations of valence electron states thus, saving a significant amount of computational time. The Hay-Wadt small-core ECPs (Ref. 31) have been adopted for Ti, Sr, and Ba atoms. The small-core ECPs replace only inner-core orbitals, but orbitals for outer-core electrons as well as for valence electrons are calculated self-consistently. Light oxygen atoms have an all-electron BS. The BS has been adopted in the following forms: O, 8-411(1d)G (the first shell is of *s* type and is a contraction of eight Gaussian-type functions, then there are three *sp* shells and one *d* shell); Ti, 411(311d)G; and Sr and Ba, 311(1d)G (see Ref. 32 for more details).

We performed calculations using the so-called *hybrid* B3PW functional (a hybrid of nonlocal Fock exchange and Becke's gradient corrected exchange functional[33] combined with the nonlocal gradient corrected correlation potential by Perdew and Wang[34]). This B3PW hybrid exchange-correlation technique was chosen because it describes very well the basic bulk properties and the electronic structure of BTO and STO perovskite crystals.[32,35] To model the above-discussed BST structures, we used the $2\times2\times2$ supercell, which consists of eight primitive STO unit cells and thus containing $5\times8=40$ atoms. Different substitutions of some Ba atoms for Sr atoms allow us to construct $Ba_cSr_{(1-c)}TiO_3$ solid solutions with different Ba concentrations. A theoretical lattice constant was optimized for each particular structure. We computed the equilibrium lattice constants for all considered superstructures and used the corresponding values of the total energies of these phases in the further study. All atoms in the supercells are fixed in their lattice sites because, according to the *ab initio* calculations,[36] the formation energies for the superstructures (at least by one order of magnitude) exceed the energy differences that define the phase competition in the ferroelectric phase transitions for the studied BST solid solutions.

The reciprocal space integration was performed by a sampling of the BZ of the supercell with the $8\times8\times8$ Pack-Monkhorst net,[37] which provides the balanced summation

TABLE II. Calculated equilibrium lattice parameters a_{eq}, and bulk moduli B for the structures (a–i) in Fig. 1 and for $BaTiO_3$ and $SrTiO_3$ (c_{st} are given in Table I).

Structure	a_{eq}, Å	B, GPa
a	3.9631	181.6
b	3.9655	180.5
c	3.9505	189.0
d	3.9445	182.3
e	3.9772	184.1
f	3.9394	184.8
g	3.9756	184.7
h	3.9262	186.1
i	3.9917	180.7
$BaTiO_3$	4.0045 (3.996)[a]	178.2 (170)[b]
$SrTiO_3$	3.9030 (3.905)[a]	192.4 (180)[b]

[a]Experiment data from Ref. 23
[b]Experiment data from Ref. 8

over the direct and reciprocal lattices.[38] To achieve high accuracy, large tolerances $N=7,87,7,14$ (i.e., the calculation of integrals with an accuracy of 10^{-N}) were chosen for the Coulomb overlap, Coulomb penetration, exchange overlap, the first exchange pseudo-overlap, and for the second exchange pseudo-overlap, respectively.[28]

IV. RESULTS FOR THE $Ba_cSr_{(1-c)}TiO_3$ SOLID SOLUTION

We choose the reference state energy in a conventional way[39] as the energy of a heterogeneous mixture, $c\mathrm{BaTiO_3}+(1-c)\mathrm{SrTiO_3}$. In our case it is calculated as the sum of weighted (according to the atomic fraction) total energies per lattice site for $BaTiO_3$ and for $SrTiO_3$. From our B3PW calculations we obtained the total energies E_{tot} and the equilibrium lattice parameter for all structures shown in Fig. 1. The equilibrium lattice parameters and the bulk moduli for these structures are collected in Table II. To illustrate the quality of our calculations, we also present the results of analogous calculations for pure $BaTiO_3$ and $SrTiO_3$. Based on the data on total energy calculations and using the definition

$$\Delta U = E_{tot} - (cE_{tot}^{BaTiO_3} + (1-c)E_{tot}^{SrTiO_3}), \tag{7}$$

we calculated the formation energies for all ordered phases shown in Fig. 1. All these energies are positive, i.e., the states in Fig. 1 and Table I have a higher energy than the reference state and thus the formation of the considered phases is energetically unfavorable at $T=0$ K with respect to the heterophase mixture $c\mathrm{BaTiO_3}+(1-c)\mathrm{SrTiO_3}$; that is, the solubility or *decomposition* of disordered $Ba_cSr_{(1-c)}TiO_3$ solid solution should occur. The data we have obtained allow us to calculate the *key energy parameter* needed for the case $T>0$. For this purpose we have chosen the phases in Figs. 1(a)–1(c) and 1(h). The magnitudes of ΔU_a, ΔU_b, ΔU_c, and ΔU_h obtained using Eq. (7) are 0.3422 eV, 0.3534 eV, 0.3581 eV, and 0.2087 eV, respectively (per a cell of the BST solid solution). When solving the set of equations

$$\Delta U_a = \tfrac{1}{2}\tilde{V}(0)c^2 + \tfrac{1}{8}\tilde{V}_1\eta_1^2, \tag{8a}$$

$$\Delta U_b = \tfrac{1}{2}\tilde{V}(0)c^2 + \tfrac{1}{8}\tilde{V}_2\eta_2^2, \tag{8b}$$

$$\Delta U_c = \tfrac{1}{2}\tilde{V}(0)c^2 + \tfrac{1}{8}\tilde{V}_3\eta_3^2, \tag{8c}$$

$$\Delta U_h = \tfrac{1}{2}\tilde{V}(0)c^2 + \tfrac{3}{128}\tilde{V}_1\eta_1^2 + \tfrac{3}{128}\tilde{V}_2\eta_2^2 + \tfrac{1}{128}\tilde{V}_3\eta_3^2 \tag{8d}$$

for the parameters $\tilde{V}(0)$, $\tilde{V}_1$, $\tilde{V}_2$, and $\tilde{V}_3$ we get $\tilde{V}(0)=-0.149$ eV per atom in quasibinary solid solution $Ba_cSr_{(1-c)}TiO_3$; parameter c was taken equal to stoichiometric composition of the corresponding phases; and all LRO parameters were taken equal to unity. We assume also that $\tilde{V}(0)$, $\tilde{V}_1$, $\tilde{V}_2$, and $\tilde{V}_3$ are concentration independent. This assumption is based on the results of the diffuse x-ray scattering data for the alloys.[40,41]

The condition $n(\vec{r})=c_A=\mathrm{const}$ corresponds to the case of the disordered quasibinary solid solution when all LRO parameters in Eqs. (8) or (5) are zero. Substitution of $n(\vec{r})=c_A$ into Eq. (2) gives the free energy of the solution

$$F(c) = \frac{1}{2}\tilde{V}(0)c^2 + kT[c\ln c + (1-c)\ln(1-c)], \tag{9}$$

where we have omitted the index A. From simple thermodynamic considerations, it follows that an equilibrium PD remains unaffected if the free energy given by Eq. (9) is replaced by

$$F(c) = -\frac{1}{2}\tilde{V}(0)c(1-c) + kT[c\ln c + (1-c)\ln(1-c)]. \tag{10}$$

This expression includes the chemical potential and is more convenient because of its symmetry with respect to $c=\frac{1}{2}$. The PD of the quasibinary disordered solid solution $Ba_cSr_{(1-c)}TiO_3$, calculated with the help of Eq. (10), is given in Fig. 2. It has *the miscibility gap*, and the decomposition reaction takes place since $\tilde{V}(0)<0$. Although this result seems to be in contradiction with the PD (Ref. 22) actually it does not because these data[22] correspond to much higher temperatures ($\sim$1500–1700 K) where the total solubility in quasibinary solid solution occurs without a formation of ordered phases. In contrast, the decomposition occurs at relatively low temperatures where the thermodynamic measurements are very difficult because of the extremely slow kinetics of the system evolution toward the equilibrium state. The kinetics of the single-phase decomposition, as the temperature is reduced, may be controlled in this case by thermal fluctuations in the system or by some specific features of the Jahn-Teller-type interaction due to the polaron formation.[42]

The calculated PD represents the case of the *limited solid solubility* in the BST solid solution. The solubility curve (*solvus*) is shown in Fig. 2 by the bold line, whereas the dashed line is the *spinodal*. To analyze the decomposition in the

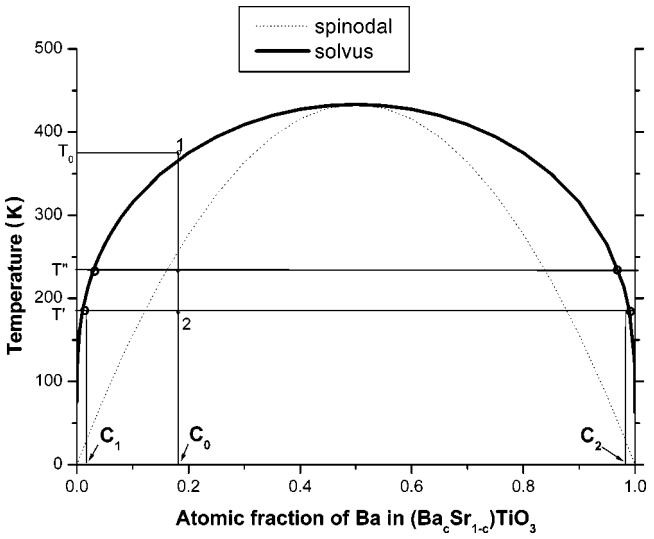

FIG. 2. Calculated phase diagram for the BST solid solution. The system is single-phase above the solvus line (point 1) and decomposes into a two-phase state below the spinodal line (point 2) at temperature T'. A line at T'' illustrates conditions leading to increase of Ba contents in a phase with low Ba concentration and to decrease of Ba contents in Ba-enriched phase.

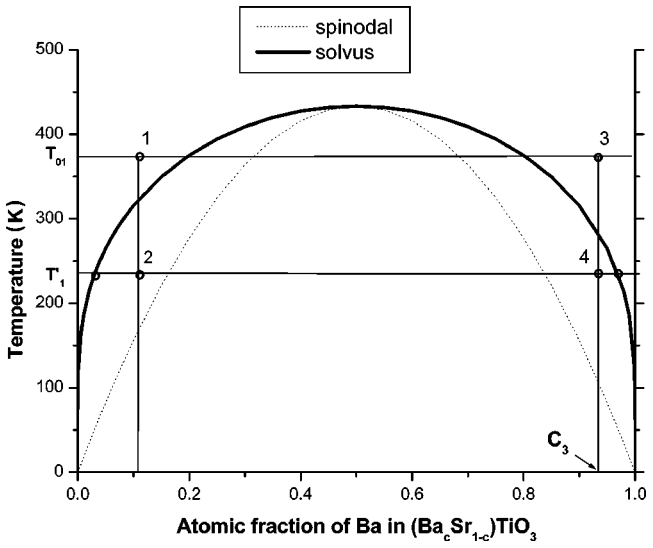

FIG. 3. Scheme illustrating the conditions of formation of Ba- and Sr-rich clusters from the disordered BST solid solution.

solid solution, let us start from point 1 in Fig. 2. This point represents the high-temperature state of a perovskite solid solution with an equilibrium concentration of Ba atoms c_0 at the temperature T_0. This is a single-phase state, corresponding to a disordered solid solution, when Ba and Sr atoms randomly occupy the sites of the simple cubic lattice, immersed in the field of the remaining crystalline lattice containing Ti and O atoms. Cooling of the system down to the temperature T' brings the system to the state *below* the spinodal, as shown by point 2.

After annealing at this new temperature T', the equilibrium two-phase state of the solid solution on this simple cubic lattice is obtained. This two-phase state is a mixture of two random solid solutions in the Ba-Sr subsystem. One phase is an extremely dilute solid solution of Ba atoms, randomly distributed in the lattice sites with the equilibrium concentration c_1 (phase 1). The second phase is also a random solid solution of the same type as the first one, but with *high* concentration of Ba atoms, c_2 (phase 2). Thus, the two-phase state represents the mixture of the two phases: one is highly enriched with Ba, whereas the second one is depleted of Ba atoms. The relative fraction of the phase 2 in the two-phase mixture is defined by the *lever rule*, and is equal to $(c_0-c_1)/(c_2-c_1)$, whereas the fraction of phase 1, with a small Ba atoms concentration, is much higher and equal to $(c_2-c_0)/(c_2-c_1)$. If the solubility regions are narrow, we have a very small fraction of phase 2, but nevertheless, it must exist.

Therefore, the two-phase state, which corresponds to the temperature T' and atomic fraction c_0, is characterized by Ba-rich regions (with Ba atomic fraction c_2) that are immersed in the Sr-enriched lattice with few Ba atoms randomly distributed on its sites. These small Ba-rich regions are also random solid solutions, but Ba concentration therein is very large and the number of Sr-occupied sites are correspondingly small. For the temperature $T''>T'$ the atomic fraction of Ba atoms in Ba-rich regions decreases, while the fraction of Sr on the sites increases in these regions.

Let us consider now the case when after cooling from the temperature T_{01} (points 1 or 3 in Fig. 3) to the temperature $T_{1'}$ the system comes to the region of the PD *between* the solvus and the spinodal (points 2 or 4 in Fig. 3). It is easy to see from Eq. (10) that the condition $d^2F(c)/dc^2>0$ is satisfied in this region of the PD. For all points c' inside this interval, the homogeneous solid solution is stable with respect to infinitesimal heterogeneity. Indeed, if $d^2F(c)/dc^2>0$, it is always possible to choose an infinitesimal region of concentrations $c_1'<c'<c_2'$ in the vicinity of the point c', where $d^2F(c)/dc^2>0$. This curve lies below the straight line connecting the points $(c_{1'},F(c_{1'}))$ and $(c_{2'},F(c_{2'}))$. Therefore, the homogeneous single-phase alloy is more stable than a mixture of two phases having infinitesimally different compositions.

If a homogeneous solid solution characterized by the condition $d^2F(c)/dc^2>0$ at point c is unstable with respect to the formation of two-phase mixture with c_α and c_β phase compositions, which are substantially different from the alloy composition, then the alloy is stable, nevertheless, with respect to an infinitesimally small composition heterogeneity. This is a *metastable* solid solution corresponding to points 2 and 4 in Fig. 3. The decomposition reaction in this case should involve the formation of *finite* composition heterogeneity. A small increase of Ba atomic fraction beyond the value c_3 (see Fig. 3) to the right of the solvus curve leaves the quasibinary solid solution in the single-phase state. The system also remains in the single-phase state if the temperature T is changed in order to bring the "alloy" to the state above the solvus. Thus, based on our analysis, we can formulate a simple thermodynamic rule of how to get nanoparticles of $BaTiO_3$ in $SrTiO_3$ even if the Ba atomic fraction in $Ba_cSr_{(1-c)}TiO_3$ is very small (Sr-rich side of the PD). The Ba-rich compact clusters will arise at low Ba composition if

the cooling process is such that, at the end, the $Ba_cSr_{(1-c)}TiO_3$ system comes into the region of the PD between the solvus and spinodal, with its subsequent decomposition in a two-phase state. A more complicated wormlike or percolation structure will be obtained if, after cooling, the system finds itself in the region below the spinodal on the PD.

At high temperatures (>400 K), alloying by Ba atoms will leave the system in the one-phase state, namely, a disordered Ba—Sr quasibinary solid solution immersed as a simple cubic Ising lattice in the lattice of the remaining crystal (i.e., in the lattice formed by Ti and O atoms). It is difficult to reach thermodynamic equilibrium in this single-phase state at low temperature because the solubility region at rather low temperature T_1' in Fig. 3 is extremely narrow. The decomposition reaction for low Ba concentration in $Ba_cSr_{(1-c)}TiO_3$ involves the formation of finite composition heterogeneity and follows the cluster formation mechanism. Particles of the Ba-rich phase formed in this region of PD are well separated. They have low connectivity and may be considered as isolated $BaTiO_3$ nanoclusters. The number of Sr atoms in these clusters is extremely small. This situation is typical for the decomposition of a binary dilute solid solution with a limited solubility.[43,44] The analogous decomposition with the formation of Sr-rich particles occurs also at the Ba-rich side of the PD. In the thermodynamic analysis of a cluster of given size, one is interested neither in the history of its appearance nor in its time evolution. We consider the cluster as a static formation, which is in a partial or complete thermodynamic equilibrium with the ambient old phase.

The spinodal decomposition in $Ba_cSr_{(1-c)}TiO_3$ solid solution means that at low temperatures and small Ba-atomic fractions there exist clusters in the old phase that consist of a large number of Ba atoms (i.e., we have clusters of "almost-pure" $BaTiO_3$ in almost pure $SrTiO_3$). In contrast, when the Ba-atomic fraction in BST is large, we may obtain (at low temperatures) the clusters of almost pure $SrTiO_3$ in almost pure $BaTiO_3$. Keeping in mind the discussed changes of the morphology in the $Ba_cSr_{(1-c)}TiO_3$ system, as the temperature decreases or the atomic fraction is varied, we may connect the real experiment facts on the ferroelectric phase transitions with the spinodal decomposition in this perovskite alloy.

V. INTERPRETATION OF AVAILABLE EXPERIMENTS

As we mentioned in the Introduction, the $SrTiO_3$-type AFD phase exists up to the critical Ba concentration $c_{cr} \sim 0.094$ (Ref. 9), which separates the PD into the two regions, one with AFD phase transition ($c < c_{cr}$) and another with the sequence of three $BaTiO_3$-type ferroelectric phase transitions ($c > c_{cr}$). As one may see from Fig. 2, we predict that at $T_{cr} \approx 100$ K the transition takes place from the structure with Ba-enriched $BaTiO_3$ clusters embedded into almost perfect $SrTiO_3$ matrix (the region between the solvus and spinodal) to the percolated, wormlike, loose structure (existing below the spinodal, where these ferroelectric transitions may occur). At the same time, the observed[9] *local polarization* inside the nonferroelectric AFD phase, according to our approach, could be related to the *formation of small Ba-rich individual clusters that are formed in the region between the solvus and spinodal*. This justifies the assumption made in Ref. 9 and the measured, therein, magnitude of spontaneous polarization in dilute $Ba_cSr_{(1-c)}TiO_3$, which is comparable to that observed in the ferroelectric phases of Ba-rich compounds. It worth noting in this context that the number of Ba-rich clusters on the left side of the PD and their fine structure strongly depend on the regime of temperature decrease and may affect a whole pattern of phase transitions in this region. For example, if these clusters are very (approx. several nanometers) small and their number is large, the ferroelectric phase transitions are sufficiently damped by the external pressure on these clusters from the Sr-rich matrix. This pressure is caused by the 2.5% mismatch of the $BaTiO_3$ and $SrTiO_3$ lattice parameters. The glassy state[8] formed at very low temperatures (<20 K) and at very small Ba concentration ($c < 0.035$) in $Ba_cSr_{(1-c)}TiO_3$ perovskite solid solution may be associated with the cluster-type morphology of the solid solution between the spinodal and binodal, in the very bottom at the left corner of the PD in Fig. 2. In this context, the question[8] "is it really important to have off-center impurity ions for glasslike behavior in these systems" has a special sense. Actually, we may have a specific morphology of the BST solid solution, analogously to dilute Ising ferromagnetics (e.g., Ref. 45) that may be interpreted as the glassy state with ferroelectric properties induced by the off-center impurities, which are sufficiently suppressed by the surrounding matrix pressure. On the contrary, in BST the mechanism of quadrupole moment formation due to elastic strain induced by the lattice mismatch between the Ba-rich regions and STO matrix may be predominant.

Our results combining alloy thermodynamics with *ab initio* calculations, are also supported by the experimental data[10] where the existence of polar Ba-rich nanoregions in dilute $Ba_cSr_{(1-c)}TiO_3$ thin films was evidently proved. It was shown that the BST film lattice dynamics is remarkably similar to that observed in the PMN relaxor ferroelectric. In relaxors the formation of polar nanoregions is caused by the compositional heterogeneity.[46] As follows from our results, analogous heterogeneity may also arise in BST. This happens at relatively low temperatures, and formation of Ba-rich clusters is just the result of the BST spinodal decomposition. Thus, the formation of polar nanoregions in BST is not necessarily associated with the presence of oxygen vacancies causing the TO phonon hardening. In fact, this may be also stimulated by the external pressure on $BaTiO_3$ clusters immersed into $SrTiO_3$ matrix. The fact that analogous effect was not observed in the BST bulk single crystals may be explained by the freezing down the kinetics of such cluster formation in the corresponding measurements or cluster number was not sufficient to find interaction of Ba-rich nanoregions, as it occurs in the film. At the same time, from the microscopic point of view, the BST film of the thickness about 1 μm (Ref. 10) contains about 2.5×10^3 cubic cells in the height and thus is thick enough to be considered as a media where the spinodal decomposition may occur.

In our nonempirical study of the PD for quasibinary $Ba_cSr_{(1-c)}TiO_3$ perovskite solid solution we consider actually

the *ground-state* energies of the competing *cubic* phases, and a reasonable question arises as to what extent the neglect of the ferroelectric transitions to the low-temperature *noncubic* phases is significant and how it may affect our predictions. To answer this question, we should remind that the formation energies, ΔU in Eq. (8) define the competition of the ordering and decomposition processes. These values are $\sim 0.2-0.35$ eV, while as follows from recent *ab initio* calculations[36] the values of the total energy differences between cubic, tetragonal, and rhombohedral structures in $BaTiO_3$ are only $0.035-0.008$ eV per cell (i.e., at least, one order of magnitude smaller). Analysis of the potential energy surfaces of atomic displacements for Ba and Ti in $BaTiO_3$ (Ref. 47) shows also that the corresponding potential barriers for Ti$\langle 001\rangle$ and Ti$\langle 111\rangle$ displacements do not exceed 0.02 eV, and for Ba$\langle 001\rangle$ displacements the potential energy surface is a single well. For incipient $SrTiO_3$ the potential energy surface has naturally the single-well shape for Ti$\langle 001\rangle$, Ti$\langle 111\rangle$, and Sr$\langle 111\rangle$ displacements. These data justify our consideration.

From the analysis of the PD obtained in our calculation, it follows also that in the case of $Ba_cSr_{(1-c)}TiO_3$ perovskite solid solution close to the point $c \approx 1$, the analogous decomposition should occur with the formation of Sr-rich clusters immersed in Ba-rich $BaTiO_3$ matrix. More details on the spinodal phase separation and the additional effects caused by such a decomposition one may find, for example, in Ref. 47.

VI. CONCLUSIONS

In this paper, we have developed a thermodynamic formalism based on *ab initio* electronic structure calculations and applied it to the $Ba_cSr_{(1-c)}TiO_3$ perovskite solid solutions. The characteristic feature of our approach is that we consider ordered structures on the Ba—Sr simple cubic sublattice. Although these artificial structures are unstable with respect to the decomposition, the relevant total energy calculations allow us to extract the necessary energy parameter, the Fourier transform of the mixing potential $V(0)$, and to predict the PD for this system. Our approach applied to the $Ba_cSr_{(1-c)}TiO_3$ system enabled us to predict the conditions under which the Ba and Sr atom distribution is either expected to be random, or Ba atoms aggregate into clusters, thus, forming Ba-rich complexes of almost pure $BaTiO_3$. We have demonstrated that the *spinodal decomposition* could serve as the universal mechanism of the nanocluster formation. As follows from our study, such nanoregions may be formed even in extremely dilute $Ba_cSr_{(1-c)}TiO_3$ if the temperature is lowered down in such a way that the system comes to the region between the solvus and spinodal in the PD of the perovskite solid solution. The decomposition is driven by the thermodynamics of the considered system. Similar decomposition in Ba-rich region of $Ba_cSr_{(1-c)}TiO_3$ allows us to predict the formation of almost pure $SrTiO_3$ nanoregions as the temperature decreases. Our theory gives theoretical justification to several key experiments, including the glass formation at low Ba concentrations,[8] the existence of polar Ba-rich nanoregions.[10] and local polarization inside the nonferromagnetic AFD phase.[9] The changing morphology of the solid solution, as the temperature and/or composition of the alloy is varied, can affect the whole pattern of ferroelectric or FD phase transitions in $Ba_cSr_{(1-c)}TiO_3$. Our theory could be applied to many other perovskite systems, in order to predict conditions for a random A-B atom distribution or for A (or B) atom aggregation into clusters, formation of A/B-rich complexes with corresponding ferroelectric properties, even when the atomic fraction of these atoms in the solid solution is small.

ACKNOWLEDGEMENT

EK and SD were financially supported by the German-Israeli Grant No. G-703.41.10.

[1] M. A. Akbas and P. K. Davies, J. Am. Ceram. Soc. **81**, 670 (1998).
[2] S.-E. Park and T. E. Shrout, J. Appl. Phys. **82**, 1804 (1997).
[3] K. Abe and S. Komatsu, J. Appl. Phys. **77**, 6461 (1995); S. Ezhivalavan and T.-Y. Tseng, Mater. Chem. Phys. **65**, 227 (2000).
[4] S. Kawashima, M. Nishida, I. Ueda, and H. Ouchi, J. Am. Ceram. Soc. **66**, 421 (1983).
[5] K. Matsumoto, T. Hiuga, K. Tanada, and H. Ichimura, in *Proceedings of the Eighth IEEE International Symposium on Application of Ferroelectrics* (IEEE, New York, 1986), p. 118.
[6] N. Setter and L. E. Cross, J. Appl. Phys. **51**, 4356 (1980).
[7] N. Singh, A. P. Singh, Ch. D. Prasad, and D. Pandey, J. Phys.: Condens. Matter **8**, 7813 (1996).
[8] V. V. Lemanov, E. P. Smirnova, P. P. Syrnikov, and E. A. Tarakanov, Phys. Rev. B **54**, 3151 (1996).
[9] C. Mènoret, J. M. Kist, B. Dkhil, M. Dunlop, H. Dammak, and O. Hernandez, Phys. Rev. B **65**, 224104 (2002).
[10] D. A. Tenne, A. Soukiassian, M. H. Zhu, A. M. Clark, X. X. Xi, H. Choosuwan, Qi. Xe, R. Guo, and A. S. Bhalla, Phys. Rev. B **67**, 012302 (2003).
[11] L. Bellaiche and D. Vanderbilt, Phys. Rev. Lett. **81**, 1318 (1998).
[12] Z. Wu and H. Krakauer, Phys. Rev. B **63**, 184113 (2001).
[13] B. P. Burton and E. Cockayne, Phys. Rev. B **60**, R12542 (1999).
[14] A. J. Bell and E. Furman, Ferroelectrics **293**, 19 (2003).
[15] L. Belaiche, A. Garcia, and D. Vanderbilt, Phys. Rev. Lett. **84**, 5427 (2000).
[16] N. J. Ramer and A. M. Rappe, J. Phys. Chem. Solids **61**, 315 (2000).
[17] H. Ehrenreich and L. Schwartz, Solid State Phys. **31**, 149 (1976).
[18] I. Grinberg, V. R. Cooper, and A. M. Rappe, Phys. Rev. B **69**, 144118 (2004).
[19] S. V. Halilov, M. Fornari, and D. J. Singh, Appl. Phys. Lett. **81**, 3443 (2002).
[20] H. Tanaka, H. Tabata, K. Ota, and T. Kawai, Phys. Rev. B **53**, 14112 (1996).

[21] L. Belaiche, Curr. Opin. Solid State Mater. Sci. **6**, 19 (2002).
[22] M. McQuarrie, J. Am. Ceram. Soc. **38**, 444 (1955).
[23] *Crystal and Solid State Physics*, edited by T. Mitsui, S. Nomura, M. Adachi *et al.*, Landolt-Börnstein, New Series, Group III, Vol. 16, Sub-Volume A (Springer-Verlag, Berlin, 1981), pp. 400–449.
[24] A. G. Khachaturyan, *Theory of Structural Transformations in Solids* (Wiley, New York, 1983).
[25] E. M. Lifshitz, J. Phys. (Moscow) **7**, 61 (1942); **7**, 251 (1942).
[26] L. D. Landau and E. M. Lifshitz, *Statistical Physics*, 2nd Revised and Enl. ed. translated from the Russian by J. B. Sykes and M. J. Kearsley (Oxford, Pergamon Press, 1978), p. 433.
[27] J. W. Christian, *The Theory of Transformations in Metals and Alloys*, Part I: *Equilibrium and General Kinetic Theory* (Pergamon Press, Oxford, 1975).
[28] V. R. Saunders, R. Dovesi, C. Roetti, M. Causa, N. M. Harrison, R. Orlando, and C. M. Zicovich-Wilson, *CRYSTAL'98 User's Manual* (Universita di Torino, Torino, (1998); http://www.chimifm.unito.it/teorica/crystal/crystal.html; http://www.cse.clrc.ac.uk/cmg/crystal
[29] R. Dovesi, R. Orlando, C. Roetti, C. Pisani, and V. R. Saunders, Phys. Status Solidi B **217**, 63 (2000).
[30] C. M. Zicovich-Wilson, R. Dovesi, and V. R. Saunders, J. Chem. Phys. **115**, 9708 (2001).
[31] P. J. Hay and W. R. Wadt, J. Chem. Phys. **82**, 270 (1984); **82**, 284 (1984); **82**, 299 (1984).
[32] S. Piskunov, E. Heifets, R. I. Eglitis, and G. Borstel, Comput. Mater. Sci. **29**, 165 (2004).
[33] A. D. Becke, J. Chem. Phys. **98**, 5648 (1993).
[34] J. P. Perdew and Y. Wang, Phys. Rev. B **33**, 8800 (1986); **40**, 3390 (1989); **45**, 13244 (1992).
[35] E. Longo, E. Orhan, F. M. Pontes, C. D. Pinheiro, E. R. Leite, J. A. Varela, P. S. Pizani, T. M. Boschi, F. Lanciotti, Jr., A. Beltran, and J. Andres, Phys. Rev. B **69**, 125115 (2004).
[36] Zh.-X. Chen, Y. Chen, and Y.-S. Jiang, J. Phys. Chem. B **106**, 9986 (2002).
[37] H. J. Monkhorst and J. D. Pack, Phys. Rev. B **13**, 5188 (1976).
[38] T. Bredow, R. A. Evarestov, and K. Jug, Phys. Status Solidi B **222**, 495 (2000).
[39] L. Kaufman and H. Bernstein, *Computer Calculations of Phase Diagrams* (Academic Press, New York, 1970).
[40] S. V. Semenovskaya, Phys. Status Solidi B **64**, 291 (1974); S. V. Semenovskaya and D. M. Umidov, *ibid.* **64**, 627 (1974).
[41] S. Semenovskaya and A. G. Khachaturyan, Phys. Rev. B **51**, 8409 (1995); *ibid.* **54**, 7545 (1996).
[42] G. Borstel, R. Eglitis, E. A. Kotomin, and E. Heifets, Phys. Status Solidi B **236**, 253 (2003).
[43] C. N. R. Rao and K. J. Rao, *Phase Transitions in Solids* (McGraw-Hill, New York, 1978).
[44] J. W. Cahn, J. Chem. Phys. **42**, 93 (1965).
[45] J. M. Ziman, *Models of Disorder. The Theoretical Physics of Homogeneously Disordered Systems* (Cambridge University Press, Cambridge, England, 1979).
[46] L. E. Cross, Ferroelectrics **76**, 241 (1987); **151**, 305 (1994).
[47] K. Binder and P. Fratzl, *Spinodal Decomposition*, in *Phase Transformation in Materials*, edited by G. Kostorz (Wiley-VCH, Weinheim, 2001), p. 411.